Extended Methodology

Oxygen Fugacity

Boivin and Bachelery (2009) used direct measurement of intrinsic oxygen fugacity and olivine-liquid equilibrium on samples of PdlF lavas whose emission temperature is known. Their values range from 3 log units below to 1 log unit above the NNO buffer.

Studies of Hawaiian magmatism (e.g., Huebner and Sato, 1970), which is comparable to that of PdlF, show that the oxidation state of Hawaiian lavas generally lies at the quartz-fayalite-magnetite (QFM) buffer (NNO-1). In contrast Rhodes and Vollinger (2005) conclude that near-vent lavas, or those that have been rapidly quenched, are likely to be nearer the magnetite-wustite (MW) buffer. In evaluating which scenario was more likely at PdlF and relevant to our samples, we considered the timing of diffusion and the vent location for the 2002 lava flow.

When observing the textures of the olivine grains, it is not uncommon to find groundmass plagioclase crystals that appear to have occluded Fe-Mg inter-diffusion from the crystal exterior. This feature is illustrated in the figure below. Groundmass plagioclase probably formed before significant olivine diffusion or any subsequent overgrowth had started, meaning that our temperatures via the Helz and Thornber (1987) geothermometer are maxima, and there has been an opportunity for transport of crystals within the melt, cooling and crystallisation to occur within the lava flow. A detailed study of the 2002 eruption by Longpré et al. (2006) observed that during the lava effusion phase, eruptive activity was rapidly focused at the main vent at 1540 m altitude. The location of RU0701 is at 69 m altitude, ~ 5.4 km distance from the vent. This suggests that the more oxidising value of the NNO+1 buffer is appropriate for our modeling purposes, as the modelled process is a demonstrably late-stage phenomenon in these samples.

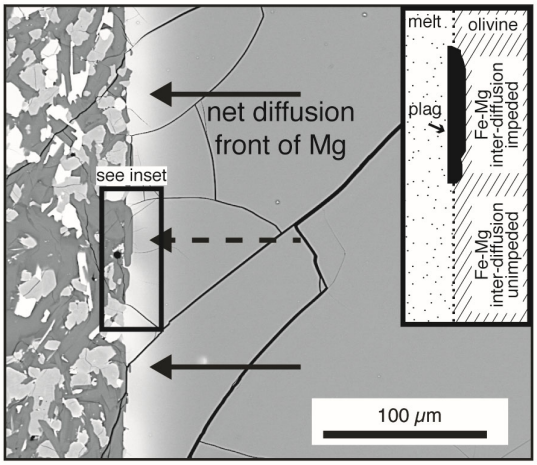

Example of occluded diffusion. A BSE image shows the effect of a plagioclase crystal that has either nucleated and grown or come into contact with the edge of an olivine. The timing of this contact was either before the onset of diffusion, or early in the period of diffusive exchange of Fe and Mg ions. Olivine immediately inboard of the plagioclase (highlighted by the dashed arrow) exhibits darker greyscale colour (more Fo rich). Diffusion is interpreted to have proceeded unimpeded around the ends of the plagioclase where the olivine was in direct contact with the 'melt', indicated by the lighter greyscale colour – higher in Fe (highlighted by the solid arrows, see inset).

X-Ray Microtomography (XMT)

The core from RU0701 was scanned using a Nikon XT H 225 X-ray microcomputed tomography (XMT) system at the Research Complex at Harwell, Didcot, UK. For each of four circular scans taken with ~20% overlap down the core, a nominal maximum energy of 70 kV was used to take 3154 projections around 360°. A 1.0 mm Al filter was used to minimise beam hardening artefacts. Standard back-filtered projection methods were used to reconstruct 16-bit 3D tiff files using identical maxima and minima to bin the raw data. These were then cropped to remove the overlap, and concatenated to form a single 3D image, and

binned to 8 bit using *ImageJ* (Schneider et al., 2012).The length of the core is the z-axis; circular cross sections are in the xy plane.

A 3D non-local means filter within the *Avizo* suite (see *www.thermofischer.com*) was then used to de-noise the image, which aided later segmentation of different phases while avoiding blurring the appearance of crystal boundaries that results from using other filtration methods (Darbon et al., 2008; Buades et al., 2011). Subtle shifts in average greyscale (1-2 levels of 256) can be detected across the concatenated boundaries, which may indicate that the response function of the XMT system drifted slightly over a period of several hours. In our case, these shifts are negligible with respect to our goal of segmenting 'olivine' from 'not-olivine', although would have a detectable influence on the determination of composition using the attenuation data (Pankhurst et al., 2018a).

Constraining the initial melt composition using Petrolog3

While estimates of melt composition based on area analysis of the groundmass were able to bracket temperatures, we take a different approach here due to the presence of overgrowth on olivine that must also be considered. Specifically, we need to approximate the melt composition prior to both olivine rim growth and groundmass formation. For the purposes of this exercise, we must return to a theoretical argument.

It is well-established that picritic lavas as oceanites must have assimilated olivine crystals (Welsch et al., 2013). Due to olivine loading, the whole rock composition as measured is a mixture between a carrier melt, and the olivine cargo (i.e., a cumulate). Crystal cores of olivine are uniform at Fo_{84}, and so we can consider the whole rock to be a mixture of Fo_{84} olivine and an unknown melt, which came together at some depth in the magmatic plumbing system.

We assume that due to the loading of crystals, the carrier melt will be saturated in Fo_{84} olivine after assimilation. To determine the melt composition required, we therefore extracted variable amounts of Fo_{84} olivine from the whole rock composition and assessed the olivine-melt equilibrium using the Petrolog3 software (Danyushevsky and Plechov, 2011). For the conditions of assimilation and assuming the melts are dry, we consider a depth of 5 km (1.3 kbar) as a plausible depth within the magmatic plumbing system for the melt and crystals to combine, following the proposed models of Albarède et al. (1997) and Bureau (1998).

The resulting models suggest that for assimilation at the MW buffer, the whole rock represents a mixture of 40.3% Fo_{84} olivine and 59.7% melt A (in Table 3). Melt A is saturated in Fo_{84} olivine (at 1247ºC/1 atm, 1255ºC/1.3 kb). If the assimilation is instead conducted at the NNO buffer, we require 41.7% Fo_{84}, olivine 58.3% melt B, which is saturated in Fo_{84} olivine at 1228ºC/1 atm and 1235ºC/1.3 kb.

These melts are then transferred to the surface and crystallisation is allowed to occur at effectively 1 atmosphere pressure at an oxygen fugacity of NNO+1. Petrolog3 is again used to project the crystallisation of the melt, including the equilibrium olivine composition, as well as the evolving melt composition. Phases considered are olivine, plagioclase, clinopyroxene, orthopyroxene and magnetite, reflecting the observed assemblages, with the exception of orthopyroxene – although it is present in low abundance in the Petrolog3 models.